Experimental UAV Data Traffic Modeling and Network Performance Analysis

Aygün Baltaci*‡, Markus Klügel*, Fabien Geyer*, Svetoslav Duhovnikov*,
Vaibhav Bajpai‡, Jörg Ott‡, Dominic Schupke*
* Central Research and Technology, Airbus, Munich, Germany
‡ Chair of Connected Mobility, Technical University of Munich, Munich, Germany
{*ayguen.baltaci, markus.kluegel, fabien.geyer, svetoslav.duhovnikov, dominic.schupke*}*@airbus.com*
{*bajpaiv, ott*}*@in.tum.de*

***Abstract*—Network support for Unmanned Aerial Vehicles (UAVs) is raising an interest among researchers due to the strong potential applications. However, current knowledge on UAV data traffic is mainly based on conceptual studies and does not provide an in-depth insight on the data traffic properties. To close this gap, we present a measurement-based study analyzing in detail the Control and Non-payload Communication (CNPC) traffic produced by three different UAVs when communicating with their remote controller over 802.11 protocol. We analyze the traffic in terms of data rate, inter-packet interval and packet length distributions, and identify their main influencing factors. The data traffic appears neither deterministic nor periodic but bursty, with a tendency towards Poisson traffic. We further create an understanding on how the traffic of the investigated UAVs are internally generated and propose a model to analytically capture their traffic processes, which provides an explanation for the observed behavior. We implemented a publicly available UAV traffic generator "AVIATOR" based on the proposed traffic model and verified the model by comparing the simulated traces with the experimental results.**

***Index Terms*—UAV, data traffic modeling, UAV measurements, UAV traffic, network performance analysis,**

I. Introduction

Recent advancements in aerial industry toward small-scale Unmanned Aerial Vehicles (UAVs) paved the way for a set of novel use cases in the sky. The diversity in size and shape, as well as the cost efficiency of UAVs enable new opportunities such as package delivery, public safety, and medical support. We can classify UAVs mainly as fixed-wing, rotary-wing and chopper drones [1]. Depending on the level of autonomy, these vehicles can perform fully-autonomous operations or under the control of a remote pilot. In general, the operation of UAVs can take place between 90 and 150 m altitude, according to the corresponding national regulations [2].

UAVs produce two types of communication traffic: 1) Command and Non-Payload Communications (CNPC), UAV and Remote Control (RC) exchanges control-related data [3]; 2) Payload communications, which enables mission-related sensory data transfer [3]. CNPC holds stringent communication requirements to ensure the safe operation of UAVs. Therefore, reliable and robust communication schemes are in demand to ensure flawless operations and public safety.

Although a number of research investigations studied UAV communication requirements on a conceptual level [4], [5] and the flight effects on the communication performance [6], [7], studies did not empirically assess the properties of the data traffic between UAV and RC. This paper provides a measurement-based analysis on the CNPC of commercial UAVs. Our aim is to determine the communication demands and to characterize the data traffic produced by the CNPC. This way, we can identify and model the individual contributors to the data traffic of the CNPC, and anticipate the requirements to design reliable UAV communications. Our particular contributions are that we characterize the CNPC traffic of three different UAVs towards their RC in terms of data rate, inter-packet interval and packet length distributions and study the end-to-end data rate, latency and transmission reliability performance. We identify the influencing factors on the traffic generation and CNPC performance, and study their effects. We model the data traffic of the UAVs and provide an open source data traffic generator for future UAV studies in [8].

We organized the rest of the paper as follows: Section II presents a review of the state-of-the-art literature in this topic. In Section III, we describe the measurement setup in detail. Afterwards, we discuss the CNPC performance analysis and the communication demands in Section IV. Section V presents the influencing factors on the data rate performance of UAV data traffic. In Section VI, we describe the data generation process on the investigated UAVs, and perform the data traffic modeling for data rate, inter-packet interval and packet length distributions. Finally, we discuss the limitations regarding our traffic model in Section VII and provide the outcome of this study as well as potential future works in Section VIII.

II. Previous Work

In this section, we investigate state-of-the-art work regarding the data traffic and the communication requirements of UAVs. Existing works analyze the UAV communication requirements on a conceptual level but mostly neglect measurement-based analysis and traffic properties beyond average rates and maximum delay bounds.

The International Telecommunication Union Radiocommunication Sector (ITU-R) analyzes the technical characteristics of CNPC links [9] and found out 7 kbps for Downlink (DL)

and 44 kbps data rate demands for Uplink (UL)[1] channel per UAV when controlled over satellite networks. Hayat *et al.* [5] reviewed the literature for the communication requirements and their expectations for data rate demands are 24 kbps for telemetry and 5 kbps for control data exchange. Similarly, authors of [10], [11] mention that UAVs produce between 20 and 24 kbps. Technical reports from the Telecom Engineering Centre (TEC) and 3^{rd} Generation Partnership Project (3GPP), [12], [4], state the data rate demands to range from 60 kbps up to several hundreds of kbps per UAV for CNPC.

Concerning latency, the studies, [13], [5], [14], estimate $40 - 100$ ms demand to control UAVs in real-time. Comparably, authors of [15] measured the latency ca. 60 ms in an experiment for Beyond Visual Line-Of-Sight (BVLoS) operations of UAVs and robots. In another experiment regarding network performance measurement of swarm UAVs [16], authors measured the end-to-end latency between 2.4 and 30 ms with varying data traffic load. Contrarily, according to [17], the latency demand ranges from 100 ms to 3 s depending on the application type.

As for reliability, 3GPP analyzes the requirements with respect to the types of communication traffic and the level of autonomy [13]. While the majority of the operations hold 10^{-3} Packet Error Rate (PER) demand, navigation messages that originate from UAV during take-off and landing require 10^{-4} PER. Similarly, Radio Technical Commission for Aeronautics (RTCA) specifies $> 99.976\%$ communication availability and $> 99.9\%$ communication continuity for CNPC [18].

Regarding the video traffic, authors of [19] propose a methodology to predict the link quality in fast moving UAVs for adaptive video streaming. They conduct real flight tests showing that their method is useful to avoid network congestion for video streaming during the movement of UAVs. When the UAV conducts video transmission, a network architecture for real-time video surveillance applications of UAVs is presented in [20]. It is based on Long Term Evolution (LTE) infrastructure with the combination of outdoor macro and indoor femto cells. The authors of [21] develop a learning-based UAV simulation framework that can test various UAV video properties using different network protocols. The trace-based measurements compare the simulation accuracy of the video quality delivery to the real-world measurements. Another study in [22] proposes an algorithm for dynamic computation offloading and control scheme to avoid video impairments on UAVs. Their experiments show improved tracking accuracy with a UAV-based video streaming.

Summarizing the presented studies anticipate the data rate requirements between 20 and 200 kbps for DL and up to 50 Mbps for UL, while the latency demand can be as low as 40 ms for CNPC. However, current studies do little to characterize drone traffic beyond average rate, latency and reliability requirements. We aim to take a step toward closing this gap in this work.

[1]Throughout this article, DL channel refers to the data traffic from Remote Control to UAV and UL channel is from UAV to Remote Control.

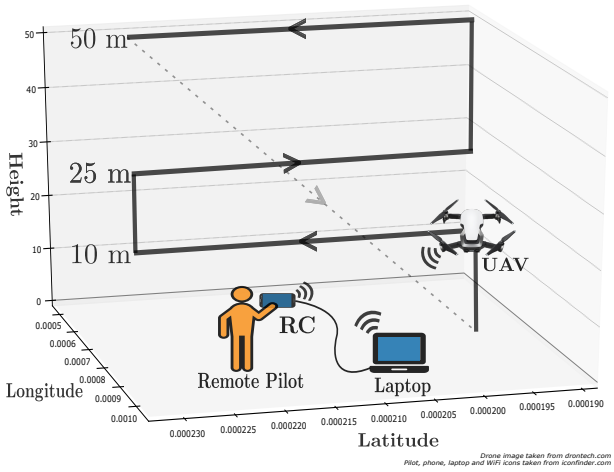

Fig. 1. Flown Trajectory in the Measurements

III. Measurement Setup

We set up a measurement campaign to obtain real data from UAV communication, with which we analyzed and modeled the UAV traffic. We compared three different UAVs from different vendors, namely the DJI Spark [23], DJI Mavic Air [24] and Parrot AR 2.0 [25], with specifications given in Table I. We selected these UAVs because they can be controlled using a smartphone, which can also be used to capture the produced data. Apart from this, all UAVs can be considered as typical representatives of their type.

We show the overall setup in Figure 1. All the UAVs use the 802.11g protocol for communication, and we took the measurements at 2.4 GHz. However, capturing the data traffic on the UAVs themselves is not possible as DJI UAVs have proprietary software. Therefore, we utilized an Android phone as Remote Control and as data sniffer to record CNPC UL and DL data on the transport layer. Concurrently, we also used a laptop with Wireless Fidelity (WiFi) card in monitor mode for data capturing on Medium Access Control (MAC) layer. We ran *Kismet* [26] and *tcpdump* [27] to capture the traffic on the phone and laptop, respectively.

We performed two types of measurements, one in the laboratory and one in-flight. We completed the in-flight measurements for network performance analysis in an outside environment, where we flew the UAVs with a pre-defined trajectory. We selected an open space, where Line-Of-Sight (LoS) condition is dominant with minor obstacles such as trees. Figure 1 shows the trajectory of the measurements taken outside. We designed this trajectory to represent all the basic movements of a UAV at varying altitudes in order to maintain our findings as general as possible. 50 m is the maximum flight altitude allowed by the software of UAVs [23]. We also flew the UAV randomly without following a trajectory but kept them outside the scope of this study. We share a sample data trace of one of those flights in [8] for interested readers.

We collected multiple measurements with each UAV to in-

TABLE I
SPECIFICATIONS OF THE UAVS USED IN THE MEASUREMENT

UAVs/Specs	DJI Spark [23]	DJI Mavic Air [24]	Parrot AR 2.0 [25]
Sensors	GPS/GLONASS 2 x 3D Infrared Module	GPS/GLONASS Altitude Sensor Fwd. & Bwd. Distance Meas. Sensor	Gyroscope Accelerometer Magnetometer Press. & Altit.
Camera	Vertical Camera Gimbal Camera - 1080p 30 fps 24 Mbps	Gimbal Camera - 4K Ultra HD 100 Mbps	Vertical Camera - QVGA 60 fps HD Camera 720p 30 fps
Max. Tx. Power	18 dBm	19 dBm	N/A

crease the confidence level of the captured data. The captured CNPC traffic comprises: 1) The control commands on the DL channel; 2) Real-time video stream; and 3) Telemetry data on the UL channel. Therefore, this measurement campaign adequately represents a remote-piloting scenario, where the remote-pilot requires a real-time video stream to maneuver the UAV. We performed both manual control and waypoint-based flights during the outside measurements for network performance analysis. This way, we could measure the effects of the autonomy level of UAVs on the communication demands.

We conducted the in-lab measurements to capture the traffic generation characteristics with minimal external effects such as wireless channel influence. During these measurements, we kept each UAV stationary in the lab and in close proximity of around 50 cm to the RC. This distance is sufficiently larger than the near-field distance of 16 cm, within which the channel can produce disturbing effects, but small enough to avoid significant impact of channel attenuation. To create comparable situations for the video stream in the in-lab and outside measurements, we set the camera of the UAV to watch a video recorded during an outside flight.

We captured User Datagram Protocol (UDP) and 802.11g packets using the Android phone and the WiFi card of the laptop in monitor mode, respectively. 802.11g packets contain the Radio Signal Strength Information (RSSI) information on UL channel, and we can analyze PER as these packets contain Packet Sequence Number (PSN) information in the data header. On the other hand, capturing UDP packets right at the interface of the RC is favorable to observe the actual packet generation rates on DL as well as the packet lengths without WiFi overhead. On UL, Radio Frequency (RF) channel conditions, MAC back-off mechanism, retransmissions and similar factors influence the packet arrival rates.

Beside the collected data, the RCs generate a log file per flight based on the telemetry data received from the UAV. The file contains the localization data from Global Positioning System (GPS) as well as Inertial Measurement Unit (IMU) sensor information such as altitude, speed, and UAV-RC distance. We also utilize this data in relating the data traffic performance to the flight status of the UAVs.

IV. NETWORK PERFORMANCE ANALYSIS

In this section, we present the CNPC performance analysis on the captured data traffic between UAV and RC. We performed the measurements in an outside environment with the pre-defined trajectory described in Section III. Parrot AR 2.0 is not included as it cannot complete the trajectory at 50 m altitude. We provide the results in terms of end-to-end data rate, inter-packet interval and transmission reliability. As we collected the data traces at the network interface of the RC, only the results of the UL channel include the effects of the RF channel conditions. Also, we captured the data for computing transmission reliability and RSSI on the laptop.

We flew DJI Mavic Air manually and DJI Spark manually as well as with waypoints. Although the increased level of autonomy with waypoints already implies less communication [28], we wanted to verify this expectation with an already-available UAV on the market. In the box graphs, we rounded the height measurements to the nearest 10 m.

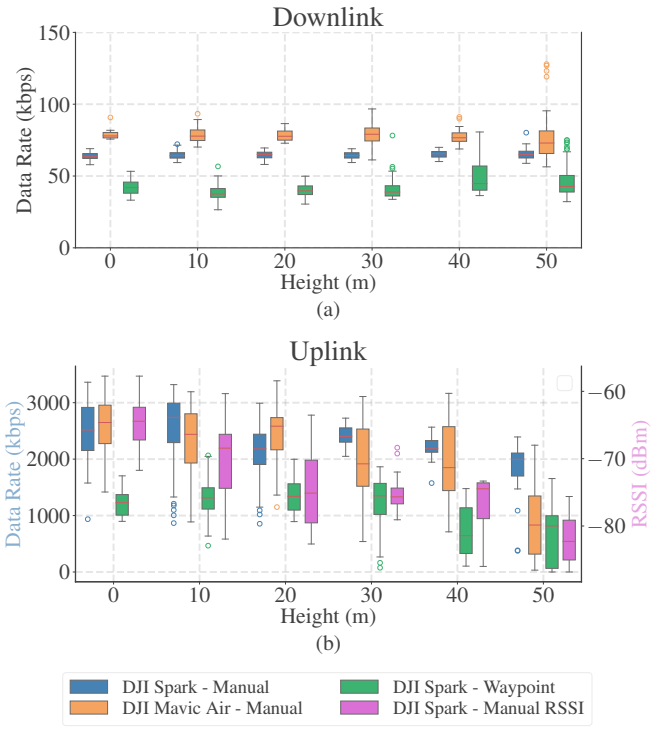

Fig. 2. Data rate results. While DL performance is stable at every altitude, performance degradation can be observed on the UL channel due to limited capacity at higher altitudes.

A. Measurement Results

We computed the data rates and inter-packet intervals rates using the timestamps of the UDP packets, and we estimated the PERs based on the PSNs of 802.11g packets. We reordered the captured packets according to their PSNs and detected the lost packets. Although PER calculations may be prone to errors with this method due to late arrivals, it still provides a useful analysis to assess the reliability performance. Finally, we repeated the measurements multiple times to increase the confidence level on the captured data. We presented the results from the most stable flying conditions.

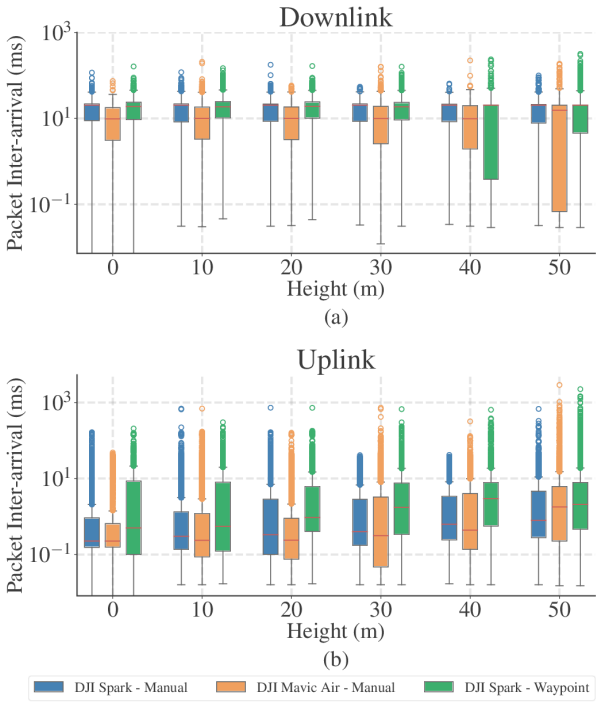

Fig. 3. Inter-packet interval results. Similar to the data rate performance, inter-packet interval rates increase at higher altitudes on the DL channels.

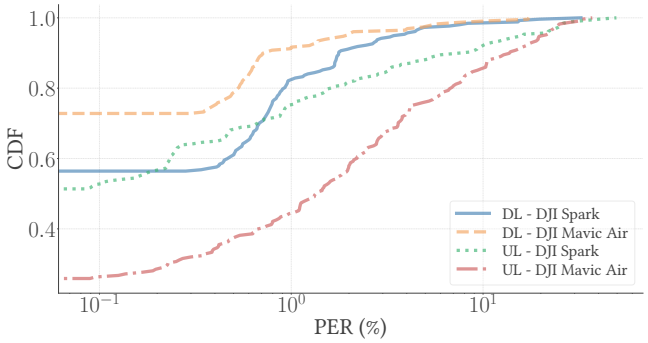

Fig. 4. Packet error rate results during manual control. Such large rates imply that lower transmission reliability levels than what is required in [13], [18] can still be sufficient to maintain the control of the UAVs.

TABLE II
OVERALL RESULTS IN DL CHANNEL WITH MANUAL CONTROL

Median/Maximum	**DJI Spark**		**DJI Mavic Air**	
Data Rate (kbps)	64.35	|| 80.19	77.67	|| 127.87
Inter-packet Interval (ms)	20.27	|| 177.33	10.26	|| 223.22
PER (%)	0	|| 32.39	0	|| 17.36

$x||y$: x and y represent the median and maximum rates of the measurements, respectively.

1) Data Rate Analysis: Figure 2 shows the results of the data rate performance. On DL, the rate is usually constant since the control commands are sent over periodic intervals. The data rate can vary between 60 and 120 kbps.

In UL, the average data rate is within $2-3$ Mbps range. It is negatively correlated with the flight altitude, especially for DJI Mavic Air. At 50 m height, the data rate drops down to 1 Mbps. The negative correlation is due to the degraded RF channel quality at higher altitudes. We observe that the average RSSI of DJI Spark reduces below -80 dBm at 50 m height. Concerning waypoint-based control, the data rate on the UL is lower compared to the manual control. The average data rate decreases from 2.4 Mbps to 1 Mbps due to the less number of video packets during waypoint-based control.

2) Inter-Packet Interval Analysis: *Inter-packet interval* is the elapsed time between the generation or arrival of two consecutive packets at the RC. It can give an insight on traffic intensity, packet latency and the generation rate of the source application. Figure 3 presents the inter-packet interval results. On DL, it stays approximately between 10 and 20 ms for both UAVs. At 50 m altitude, inter-packet intervals go up to 258 ms, which is due to poor channel performance.

As for UL, the intervals are less stable and larger compared to the DL. This effect is caused by varying delays when exceeding the channel capacity with large data rates on the UL, as RF conditions are worsened at higher altitudes. Maximum inter-packet interval goes up to 3 s on DJI Mavic. When the packet arrival exceeds a certain threshold, the RC application considers a loss of communication and notifies the pilot. However, the UAV maintains its current position. While the average inter-packet interval is 3.3 ms on UL with manual control, it increases to 8.34 ms in waypoint control, since the frequency of the video packets decreases.

3) Packet Error Rate Analysis: For PER measurements, we present the portion of the captured data when the communication link is not lost. Figure 4 shows the PER results only for manual control since we did not capture 802.11g packets to compute PER during flights with waypoint-based control. For DL, the average PER is 0.72% for both UAVs, while the maximum PER is 32.39%. As for UL, PER is worse due to the increased number of packets and consequently the larger capacity demand. Nonetheless, the average PER is 3.37%.

We present the overall results of DL and UL channels in Table II and Table III, respectively. The maximum data rate is recorded to be 128 kbps while the maximum inter-packet interval is 223 ms on DL. As for UL, the maximum data rate is 3.47 Mbps using HD video stream. Although the maximum inter-packet interval is 2.89 s, it includes the period when there is a loss of communication. Excluding the outlier inter-packet intervals on UL, we can consider ca. 250 ms from DL as the upper latency threshold for both channels.

Overall, these results provide a broad analysis regarding the communication demands and performance of the tested UAVs. The results may naturally vary for other UAVs with the number of cameras, video quality, video compression rate, computational power and so forth. Another influencing factor is the UAV level of autonomy. Fully autonomous UAVs may not require video streaming, as the they send only periodic

TABLE III
OVERALL RESULTS IN UL CHANNEL WITH MANUAL CONTROL

Median/Maximum	DJI Spark	DJI Mavic Air
Data Rate (kbps)	2302.65 || 3362.84	2116.83 || 3470.85
Inter-packet Interval (ms)	0.38 || 730.44	0.26 || 2899.89
PER (%)	0 || 49.58	1.35 || 37.14

$x||y$: x and y represent the median and maximum rates of the measurements, respectively.

updates to the ground station to verify their mission. Therefore, the data traffic pattern on UL may become symmetric to DL. Also, increasing the the level of UAV autonomy can relax the latency demands since onboard processors can handle flight-related tasks. The next section will further extend the network analysis to study the individual effects of the influencing elements on the CNPC performance.

V. INFLUENCING FACTORS ON NETWORK PERFORMANCE

The data traffic and network performance on the investigated UAVs is generally be influenced by several external factors. Firstly, the RF channel conditions fluctuate depending on the motion of UAVs as well as the physical environment. Secondly, the amount of video information on the UL channel varies based on the video encoder type, UAV movement, the lighting condition, and so on. Thirdly, the interaction with the RC might also influence the control traffic but does not show any observable effect on the investigated UAVs. All of these factors are highly situation- and implementation-dependent, and often not known, e.g., the exact settings of the video encoder may vary among different UAVs and are in general not revealed to the end user. However, we can gain a higher-level insight on the typical influence as observed on a state-of-the-art UAV in various scenarios. We use only DJI Spark in the measurements for simplicity. We show the measurement results for the UL channel to observe the effects of both the video encoder and the RF channel.

A. Effects of RF Channel and the Video Encoder

In this part, we aim at separating the effects of RF channel and the video encoder to individually analyze their influence on the data rate performance. We set up the first measurement to observe the effects of only the RF channel. As the DJI software does not allow the UAV camera to be turned off, we covered the camera to minimize the video encoder effects on the data traffic. We flew the UAV outside following the pre-defined trajectory. Afterwards, we conducted the second measurement in the lab to analyze the effects of only the video encoder as described in Section III.

Figure 5 presents the data rate performance of both investigations. Although RF channel conditions produce outliers at very low rates at 50 m height, the fluctuations are less compared to the the ones from the video encoder. DJI Spark has H.264 variable bit-rate encoder [23] and consequently, the data rate largely varies at every height below 50 m due to the constant motion of the UAV. Hence, these results show that

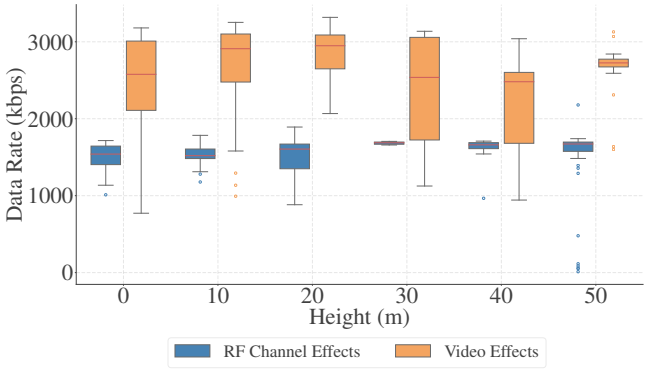

Fig. 5. Analysis of RF and video encoder effects on data rate performance. While the variable bit rate encoder causes large fluctuations, RF channel strongly affects the data rate performance, especially at 50 m.

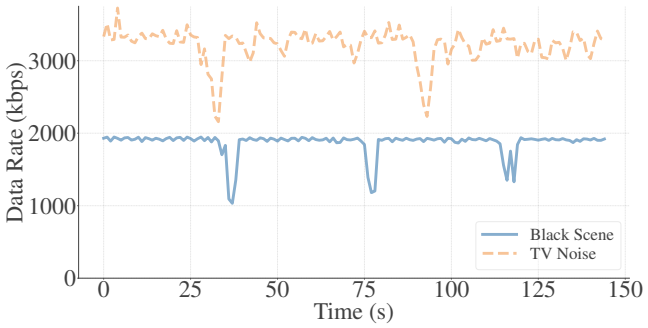

Fig. 6. Analysis of the camera scene on data rate performance, which shows the lower and upper bounds on observed data rate performance on the UL channel of DJI Spark

while RF channel can majorly affect the data rate performance under poor conditions, the variable bit-rate encoder is in fact the main cause of the large fluctuations on the data rate.

B. Effects of the Video Scenery

We performed two sets of measurements to determine the lower and upper bounds of video data rate based on the recorded scenery. For this, we used the fact that the transmitted data rate is correlated with the information level of the image scenery itself. To determine a lower bound on video traffic, we placed the UAV in a completely dark room, where the camera recorded only black pixels. This reduces the traffic sent by the encoder to a value below that one encountered in real world. For the upper bound, we set the UAV camera to watch a television noise effect, where the pixel values constantly alter and thus information level of the images is very high. As both measurements can point to the upper and lower bound of video rates, we analyze their maximum variations.

Figure 6 shows the results. The data rate has repetitive drops approximately every 40 s, which we could not fully clarify but which most probably is related to the video encoder itself. The rate varies between 1.8 and 3.3 Mbps indicating that the data rate performance can vary up to a factor of 1.8 depending on the camera scenery of the tested UAV. Moreover, the data rate

is more constant when the UAV records only black pixels. This result verifies that the change in the video scenery is the main reason of large fluctuations on the video rate.

VI. Modeling the UAV-RC Data Traffic

We present our intuition of the traffic generation process on the UAVs, which we obtained by testing different implementation options and observing the impact on the produced traffic. We propose an analytical model based on our best estimation, which can derive the data rates on DL and UL channels. Afterwards, we matched the Probability Density Function (PDF) distributions of data rate, inter-packet interval and packet length parameters of the collected data with the statistical models obtained from our analysis. As the data distributions of all UAVs have similar characteristics, which we later show in Figure 9, we present the PDF results of only DJI Spark for the sake of brevity. Based on the proposed packet generation model, we set up a Monte-Carlo simulation to validate the model against the collected data from the UAV.

A. Overview of the Packet Generation Process

Understanding the packet generation process is essential to correctly formulate and model the data traffic of UAVs. DJI UAVs have proprietary software and thus, it is not possible to access their operating systems to analyze the data generation flow. Instead, we gather an intuitive understanding on the way the traffic is generated, propose a model and verify the model by conducting a Monte-Carlo simulation study.

The overall UAV set-up and the collected traces indicate that the traffic consists mainly of control commands on DL and of a video stream along with telemetry data on UL. According to [29], each control/telemetry parameter is updated at a fixed rate and five different update rates (1, 10, 50 and 100 Hz) are possible for DJI UAVs. Although this leads to the assumption that the traffic is very deterministic and periodic, our analysis shown later in Figure 8 indicates that we cannot model the aggregate UAV traffic with a simple periodic generation process. To understand the underlying process, we implemented several options on how periodic the traffic can be generated. We present the one that leads to traffic patterns closest to the collected data from the UAV.

We model the underlying process in terms of a discrete-time system with time $t \in \{0, 1, ...\}$, where each instant refers to a small time step of fixed separation, e.g., a CPU cycle. As depicted in Figure 7, we consider a set of captured parameters $\mathcal{I}$, with parameter $i \in \mathcal{I}$, that are transmitted. A parameter may correspond to telemetry information such as position or status, or control commands. Each parameter i is read with a fixed frequency f_i and for each read, a binary value of length l_i is generated on the application layer. After generation, the value is placed into a transport layer transmission buffer. The status of the buffer is checked regularly with a fixed rate f_u, and for each value that is in the buffer, a UDP packet is created and sent to the buffer of the MAC layer for wireless transmission.

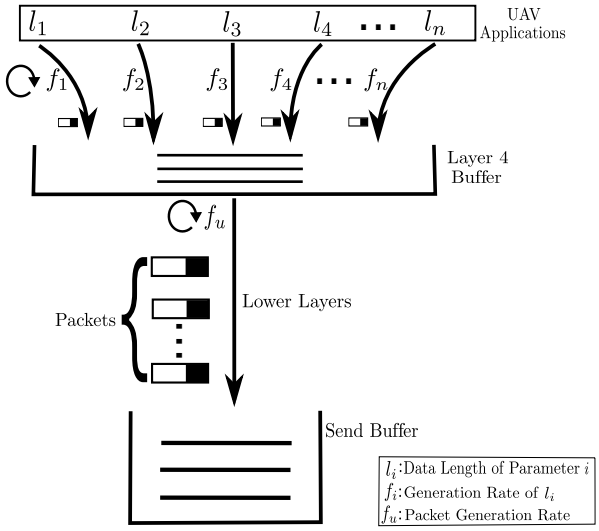

Fig. 7. Overview of the packet generation process of UAVs from the application layer down to the network interface.

With this procedure, we can model the transmissions by a combination of mathematical processes. In each time step t, parameter $i \in \mathcal{I}$ generates data $r_i[t]$ according to the equation:

$$r_i[t] = \sum_{k=-\infty}^{\infty} \delta[t - \Delta_i - kT_i] \cdot l_i, \tag{1}$$

where $k \in \mathbb{N}$ is an integer, Δ_i is an offset, $T_i = 1/f_i$ is the transmission period of parameter i and $\delta[x]$ is the Kronecker delta, which is one for $x = 0$ and zero otherwise. As can be seen, the data produced by parameter i is corresponds to a strictly periodic signal with fixed rate f_i and a "phase" offset Δ_i, where each signal peak as the same height l_i.

B. Data Rate Formulation

Using Equation 1, we model the DL and UL data rates in the following sections.

1) DL Channel: On DL, the data traffic consists only of control-related packets. Let $\mathcal{I}_{\text{dl}}$ be the set of parameters sent in DL. Then, the traffic stream aggregates their values over a time interval of T_{dl} steps and sends an own packet for each parameter of $\mathcal{I}_{\text{dl}}$ that has been generated in this interval. We model this by considering a UDP transmission buffer that holds an amount of data $B_{\text{dl}}[t]$ in step t. The buffer evolves from step to step according to the Lindleys' recursion:

$$B_{\text{dl}}[t] = \max\{B_{\text{dl}}[t-1] + \sum_{i \in \mathcal{I}_{\text{dl}}} r_i[t] - R_{\text{dl}}[t], 0\}, \tag{2}$$

where $R_{\text{dl}}[t]$ is the amount of transmitted data via the UDP socket in step t and the $\max\{\cdot\}$ operation ensures only positive values for the buffer status. $R_{\text{dl}}[t]$ is given by:

$$R_{\text{dl}}[t] = \sum_{k=-\infty}^{\infty} \delta[t - \Delta_{\text{dl}} - d_k - k \cdot T_{\text{dl}}] B_{\text{dl}}[t], \tag{3}$$

where $d_k \geq 0$ is a sequence of processing delays according to a random distribution. That is, the application space scans the buffer status regularly, at time instants that are T_{dl} apart, processes them and then sends the entire buffer content to its peers. Together, $B_{\text{dl}}[t]$ and $R_{\text{dl}}[t]$ model that $B_{\text{dl}}[t]$ aggregates the send data within a scan interval of T_{dl} steps. After these steps, the entire data is flushed toward the MAC layer in a burst. This creates the effect that although each parameter is read with a strict periodicity by itself, the overall traffic distribution below application layer becomes more complex and in particular more bursty. Finally, the time-averaged rate $\overline{R}_{\text{dl}}$ can be verified to be:

$$\overline{R}_{\text{dl}} = \lim_{T\to\infty} \frac{1}{2T} \sum_{t=-T}^{T} R_{\text{dl}}[t] = \sum_{i\in\mathcal{I}_{\text{dl}}} l_i f_i. \tag{4}$$

2) UL Channel: The UL in the tested UAVs consists of both telemetry and video streams. We model the telemetry data as set of data parameters $\mathcal{I}_{\text{ul}}$, similar to the DL parameters. In addition, we consider a video stream that creates data according to a time-dependent process $r_v[t]$. Our traces indicate that all UAVs create video streams with variable bit-rate but fixed frame-rate. The exact number of bytes per frame then may vary and is subject to various factors including the recorded scenery itself as shown. We therefore can model the $r_v[t]$ by a fixed-rate process with variable data per sample [30]:

$$r_v[t] = \sum_{k=-\infty}^{\infty} \delta[t - \Delta_v - k \cdot T_v] \cdot l_v[t], \tag{5}$$

where the data per frame $l_v[t]$ changes in time and is a function of the encoded scenery, the number N_v of pixels processed by the video encoder, the color depth D_v of the camera, the frame rate F_v and the compression rate X_v of the encoder. Various models for the evolution of $l_v[t]$ exist [30], which may be well adopted into our model assumption. However, the full analysis of the time dependence of $l_v[t]$ seen on the UAVs is out of the scope of this work. Altogether, we can model the UL data by a buffer process $B_{\text{ul}}[t]$ that evolves according to:

$$B_{\text{ul}}[t] = \max\{B_{\text{ul}}[t-1] + r_v[t] + \sum_{i\in\mathcal{I}_{\text{ul}}} r_i[t] - R_{\text{ul}}[t], 0\}, \tag{6}$$

where $R_{\text{ul}}[t]$ is the amount of data that is transmitted via the UDP socket and is given by:

$$R_{\text{ul}}[t] = \sum_{k=-\infty}^{\infty} \delta[t - \Delta_{\text{ul}} - d_k - k \cdot T_{\text{ul}}] B_{\text{ul}}[t]. \tag{7}$$

Analog to (4), the average rate simplifies to:

$$\overline{R}_{\text{ul}} = \sum_{i\in\mathcal{I}_{\text{ul}}} l_i f_i + \overline{f}_v \bar{l}_v(N_v, D_v, F_v, X_v), \tag{8}$$

where $\bar{l}_v(N_v, D_v, F_v, X_v)$ and $\overline{f}_v$ are the average packet length and frame rate of the video stream, respectively.

Algorithm 1 Simulative Data Generation Flow

```
Consider traffic direction d ∈ {ul, dl}
for every t do
    // Update parameter & control values
    for i ∈ I_d do
        if (t − Δ_i)%T_i == 0 then
            parameter[i] ← current value i
    // In uplink add video stream
    if (d == ul) and (t − Δ_v)%T_v == 0 then
        r_v ← current video frame
    // Push data out from buffer
    if (t − Δ_d)%T_d == 0 then
        for i ∈ I_d do
            if !empty(parameter[i]) then
                send_from_buffer(parameter[i])
                parameter[i] ← ∅
        if !empty(r_v) then
            send_from_buffer(r_v)
            r_v ← ∅
```

C. Verification of the Formulation

To verify the correctness of the data rate models, we created a data generator using Python [8]. Algorithm 1 shows the pseudo-code of our generation flow. Note that in Algorithm 1, we used a "switch" variable $d \in \{\text{ul}, \text{dl}\}$ to group UL and DL direction into one code, i.e., $\mathcal{I}_d$ is either $\mathcal{I}_{\text{ul}}$ or $\mathcal{I}_{\text{dl}}$ and T_d is either T_{ul} or T_{dl}. In words, Algorithm 1 states that for each parameter i, data values are added to a local variable in regular time intervals and if the direction is UL ($d == \text{ul}$), the same happens for the video frames. Also at regular time intervals but with different frequencies, the variables are checked for their status and if new values are present, these are sent out through the socket to the lower layer. Our implementation also includes packet fragmentation if the values exceed the maximum transmission unit, which is the case for video frames. As our data generation code is run in real-time on the user-space of a Linux machine, random processing delay is automatically added to the process, such that we did not explicitly account for it in the generation loop.

D. Data Traffic Model Estimation

In this part, we present the data distribution and fitting statistical models of the UAV data traffic. We also compare the distribution results from our simulation with the collected UAV data. We present the PDF distributions of data rate, inter-packet interval and packet length. We used the Mean Squared Error (MSE) to measure the similarity of the simulated data to that of the collected UAV data. We present the PDF results of only DJI Spark as the data distribution of the tested UAVs are alike, which can be observed in their Cumulative Distribution Function (CDF) distributions in Figure 9.

1) Data Rate: Figure 8 (a,e) presents the PDF results. We can describe the data rate distributions of DL and UL with a compound Poisson model. This is mainly due to the exponential distribution of the inter-packet intervals, which causes the generated packets to follow compound Poisson process over distinct time intervals. Therefore, we can describe

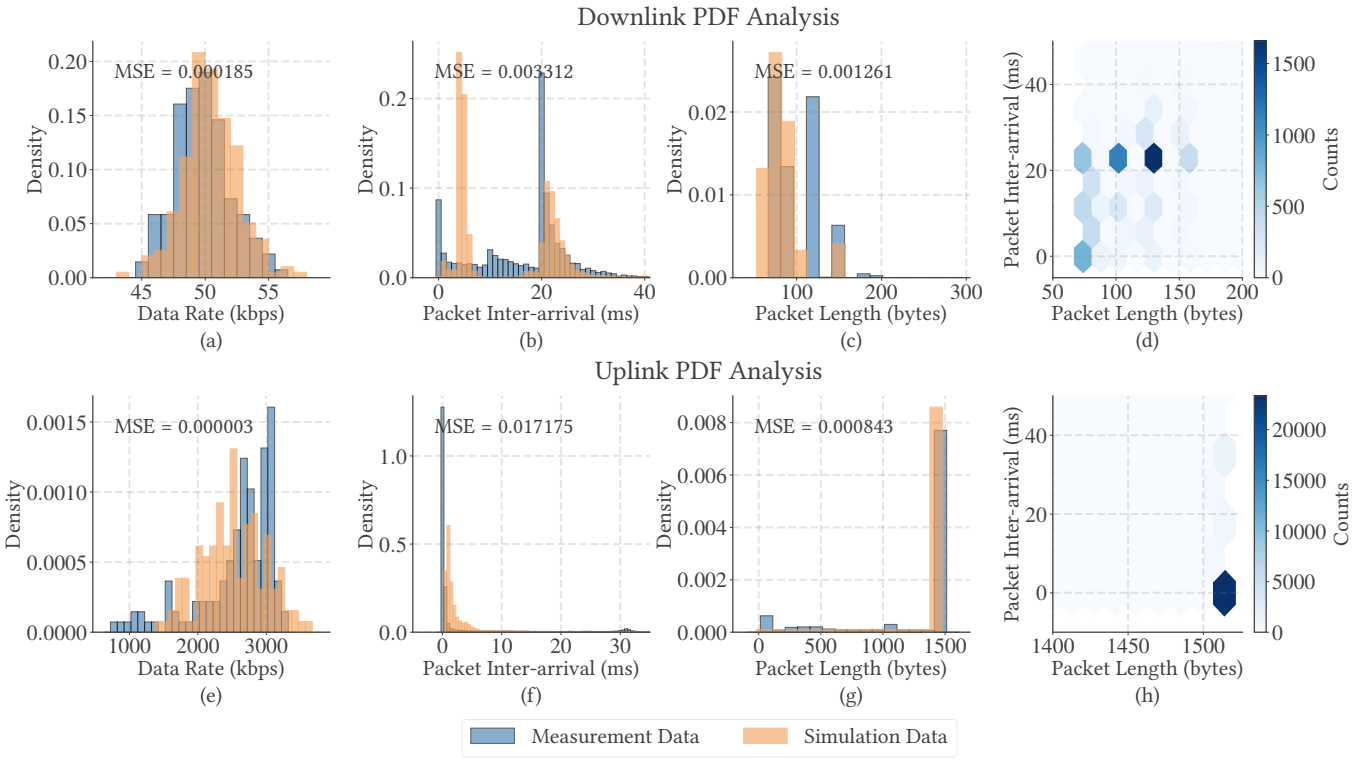

Fig. 8. PDF of the measured data from DJI Spark. The data rate (a),(e) is Poisson process, the inter-packet interval (b),(f) is exponentially distributed and the packet length (c),(g) does not follow any distribution. (d),(f) shows the correlation of inter-packet interval and packet lengths which generates the data rate distribution.

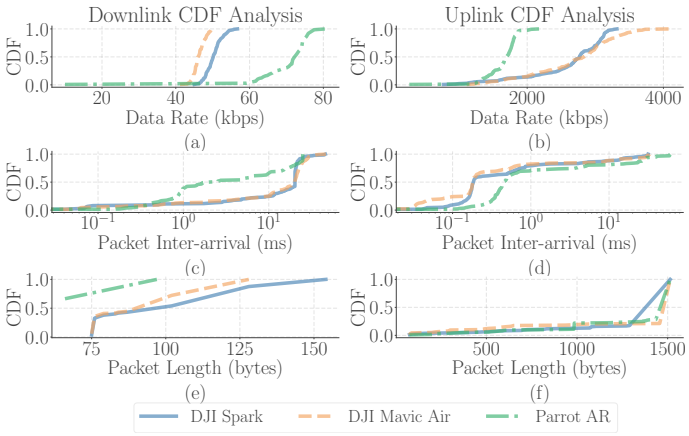

Fig. 9. CDF of DL and UL data of all the tested UAVs. The CDF patterns in each graph except (e) are related to one another, which indicates that the data traffic distributions of all the UAVs are alike.

our packet generation model with *M/G/1* queue model, where the packet arrival is Poisson [31].

We observe the Poisson process with the long tails in the graphs. On DL, the data rate only consists of independently generated control parameters. On UL, the data rate is mainly determined by the motion-dependent and bursty video traffic.

As for the simulation results, the distribution pattern has similar characteristics to that of the collected data from the UAVs on the DL channel. On UL, although the distribution is Poisson, the median rate is larger than that of the collected data. Nevertheless, the MSE of the PDFs is lower on UL since the density values are lower in the magnitude of 100 compared to that of DL.

2) Inter-packet Interval: Figure 8 (b,f) presents the results. Different parameter generation rates, f_i, and the packet generation rate, f_u from Figure 7 causes packets to appear as independently and uniformly distributed in a pseudo-random manner. Because, the inter-packet intervals follow the pattern of a Linear Congruential Generator (LCG) [32], which is known to produce pseudo-random numbers with uniform distribution. Therefore, the inter-packet interval follows exponential distribution. This model is widely inherited for the time-interval analysis of discrete events [33].

On DL, two peaks are present around 1 and 20 ms, and the distribution density then gradually decreases. The first peak around 1 ms is due to the bursty packet generation of the values that are accumulated at the buffer of the transport layer. The consecutive generation can occur when the parameter generation rate, f_i, is faster than the traffic generation rate, $f_{\text{dl}} = 1/T_{\text{dl}}$, or when values from different processes arrive within one scan interval T_{dl}. As for the second peak at 20 ms, it is the time interval between the last generated packet of the previous buffer scan and the first packet of the new buffer

scan, i.e., it is T_{dl}. The smaller peaks between 0 and 20 ms in the graph appear mainly due to the random processing times of the packets in the hardware. The intervals > 40 ms can imply the random occurrences of empty buffer scans.

With regard to UL, the majority of the packets are separated within 1 ms interval since large video information is partitioned into multiple segments in the buffer and sent consecutively. Afterwards, the density decreases and spreads, which is mainly produced by the telemetry packets.

We observe similar distributions in our simulation results. On DL, the bursty packet generation can be observed around 5 ms, which is slightly shifted compared to that of the collected UAV data. Also, the processing delay is not as widespread. On the other hand, the second peak in the simulated data is well-aligned with the actual UAV data. As for UL, the exponential decay can also be observed on the simulation but wider compared to the actual UAV data. The MSE is lower on the DL channel than that of UL.

3) Packet Length: In Figure 8 (c,g), the packet lengths are discretely separated on DL. The particular distribution shown by the measurement is due to the different generation frequency of each data parameter. The simulation result confirms this behavior in general, albeit with a different particular pattern. As for the UL, over 73% of the packets are 1514 bytes, which are the partitioned video packets. Such pattern is also observed in the data distribution of the simulation.

Figure 8 (d,h) shows the correlation between the inter-packet interval and packet lengths, and thus creates a relation to the two middle columns of the figure, identifying which packet length dominates at which inter-packet interval time. In Figure 8 (d), the distribution is spread, but the density is higher around 100 and 140 bytes ca. at 20 ms, and around 70 bytes at 0 ms. In (h), the density is concentrated on 1514 bytes at 0 ms.

We present the CDF of the collected data from all the tested UAVs in Figure 9 to show the similarities in their data distributions. In (a-d,f), the data of all the UAVs have the same pattern but the median rates of Parrot AR are different than that of DJI UAVs. In (e), the packet length distribution of Parrot AR is Bernoulli: 65.6% of packets are 66 bytes and the rest are 97 bytes. DJI Spark and Mavic Air have distinct packet length distributions between 75 and 154 bytes.

We share our UAV data traffic generator *AVIATOR* for public use in [8] along some of the collected data traces from the UAV. Future research investigations can utilize AVIATOR to generate realistic UAV data traffic in their simulation, emulation as well as hardware-based studies.

VII. Discussion on the Limitations of the Results

In this study, we used three well-known UAVs available on the market to analyze, model and generalize their generated traffic. However, although the UAVs can be seen as typical representatives of their type, there are various ways how they can be built and how their software can be structured, which also influences the produced traffic. On UL, the encoders of the UAV cameras significantly influence the generated traffic. A simple switch of the used encoder may change the induced data rates and traffic behavior, in which case our analysis might loose validity. On DL, our model is based on the assumption that packets are generated with independent but fixed periodicity for different parameters. A change to, e.g., an event-based packet generation would change the properties and hence the model. Finally, also the network type itself has an impact on the observed traffic. Current UAVs mainly communicate over random access channels, similar to WiFi standards. The back-off mechanism alone strongly influences the traffic pattern. On the other hand, a UAV that communicates over a cellular network might well produce a different behavior from the RC point-of-view.

The generated traffic from our simulation model well matches to the collected UAV traffic, as depicted in Figure 8. The model can further be improved to better align, especially the subplots (b, c, e). Nevertheless, this model approximates the main effects of the actual UAV traffic. As result, our proposed models represent typical traffic of typical UAVs that are currently available, with uncertainty whether they will be valid for future products.

Our main conclusion, however, is that the traffic generated by UAVs follows complex patterns and may have a diverse nature. The most significant insight probably is that due to the sheer number of exchanged parameters, the created traffic tends to assume known properties such as exponential inter-arrival times and exhibits bursty behavior, even if each value itself is updated in a periodic manner. This overall effect is in contrast to assumptions made in literature, which mainly consider UAV traffic to be well-behaved, according to deterministic and periodic patterns.

VIII. Conclusion

In this study, we present the results of a measurement campaign, where we analyze the data traffic between various UAVs and the RC. The network performance analysis shows that the remotely-piloted UAV operations can demand up to 130 kbps and 3.5 Mbps with the tested UAVs for DL and UL channels, respectively. Furthermore, 250 ms can be considered as the upper-bound latency threshold.

We also study how the camera scenery with H.264 encoder as well as the RF channel conditions influence the data rate performance. The constant motion of UAV causes fluctuations on the data rate and the poor RF channel conditions at high altitudes can limit the channel capacity.

Finally, we model the data rate, inter-packet interval and packet length distributions of the collected data. Our results show that the inter-packet interval is exponentially distributed and consequently, the data rate follows compound Poisson process. Packet lengths cannot be modeled as they are discrete and dependent on the number of different data parameter generation rates. The modeling results and the UAV traffic generator can be beneficial for future works to estimate the data traffic between UAV and RC. These results reflect the capabilities of only the tested UAVs. Therefore, a future study should extend this work with other types of UAVs to further evaluate their data traffic.

REFERENCES

[1] G. Singhal, B. Bansod, and L. Mathew. Unmanned aerial vehicle classification, applications and challenges: A review, 11 2018. https://doi.org/10.20944/preprints201811.0601.v1.

[2] Global Legal Research Center. Regulation of drones. Technical report, The Law Library of Congress, 2016. [Online]. Available at:https://www.loc.gov/law/help/regulation-of-drones/regulation-of-drones.pdf [Accessed on 11/01/2021.].

[3] Y. Zeng, J. Lyu, and R. Zahng. Cellular-connected uav: Potential, challenges, and promising technologies. *IEEE Wireless Communications*, 26(1):120–127, 2019. https://doi.org/10.1109/MWC.2018.1800023.

[4] 3GPP. Study on enhanced lte support for aerial vehicles (release 15). Technical Report 36.777, 2017. [Online]. Available at:https://portal.3gpp.org/desktopmodules/Specifications/SpecificationDetails.aspx?specificationId=3231 [Accessed on 11/01/2021.].

[5] S. Hayat, E. Yanmaz, and R. Muzaffar. Survey on unmanned aerial vehicle networks for civil applications: A communications viewpoint. *IEEE Communications Surveys Tutorials*, 18(4):2624–2661, 2016. https://doi.org/10.1109/COMST.2016.2560343.

[6] M. Asadpour, B. Van den Bergh, D. Giustiniano, K. A. Hummel, S. Pollin, and B. Plattner. Micro aerial vehicle networks: an experimental analysis of challenges and opportunities. *IEEE Communications Magazine*, 52(7):141–149, 2014. https://doi.org/10.1109/MCOM.2014.6852096.

[7] M. Asadpour, D. Giustiniano, and K. A. Hummel. From ground to aerial communication: Dissecting wlan 802.11n for the drones. In *Proceedings of the 8th ACM International Workshop on Wireless Network Testbeds, Experimental Evaluation & Characterization*, WiNTECH '13, page 25–32, New York, NY, USA, 2013. Association for Computing Machinery. https://doi.org/10.1145/2505469.2505472.

[8] A. Baltaci. uav communication data traffic generator (AVIATOR), January 2021. [Online]. Available at:https://github.com/aygunbaltaci/AVIATOR [Accessed on 14/01/2021.].

[9] ITU-R. Examples of technical characteristics for unmanned aircraft control and non-payload communications links. Technical Report M.2233, 2011. [Online]. Available at:https://www.itu.int/en/ITU-R/space/snl/Documents/R-REP-M.2233-2011-PDF-E.pdf [Accessed on 11/01/2021.].

[10] L. Shan, R. Miura, T. Kagawa, F. Ono, H. Li, and F. Kojima. Machine learning-based field data analysis and modeling for drone communications. *IEEE Access*, 7:79127–79135, 2019. https://doi.org/10.1109/ACCESS.2019.2922544.

[11] L. M. Schalk and M. Herrmann. Suitability of lte for drone-to-infrastructure communications in very low level airspace. In *2017 IEEE/AIAA 36th Digital Avionics Systems Conference (DASC)*, pages 1–7, September 2017. https://doi.org/10.1109/DASC.2017.8102112.

[12] TEC, Radio Division. Communication aspects of unmanned aircraft system (uas). Technical report, TEC. [Online]. Available at:https://www.tec.gov.in/pdf/Studypaper/UAV.pdf [Accessed on 11/01/2021.].

[13] 3GPP. Unmanned aerial system (uas) support in 3gpp (release 17). Technical Report TS 22.125, 2019. [Online]. Available at:https://www.3gpp.org/ftp/Specs/archive/22_series/22.125/ [Accessed on 11/01/2021.].

[14] F. Maiwald and A. Schulte. Using lte-networks for uas-communication. In *36th European Telemetry and Test Conference (ETT)*, 2016. https://doi.org/10.5162/etc2016/5.3.

[15] T. Kagawa, F. Ono, L. Shan, K. Takizawa, R. Miura, H. Li, F. Kojima, and S. Kato. A study on latency-guaranteed multi-hop wireless communication system for control of robots and drones. In *2017 20th International Symposium on Wireless Personal Multimedia Communications (WPMC)*, 2017. https://doi.org/10.1109/WPMC.2017.8301849.

[16] O. Bouachir, M. Aloqaily, F. Garcia, N. Larrieu, and T. Gayraud. Testbed of qos ad-hoc network designed for cooperative multi-drone tasks. In *Proceedings of the 17th ACM International Symposium on Mobility Management and Wireless Access*, MobiWac '19, page 89–95, 2019. https://doi.org/10.1145/3345770.3356740.

[17] Y. Zeng, Q. Wu, and R. Zhang. Accessing from the sky: A tutorial on uav communications for 5g and beyond. *Proceedings of the IEEE*, 2019. https://doi.org/10.1109/JPROC.2019.2952892.

[18] RTCA. Minimum aviation system performance standards for C2 link systems supporting operations of unmanned aircraft systems in U.S. airspace. Technical Report DO-377, Mar 2019. [Online]. Available at:https://global.ihs.com/doc_detail.cfm?item_s_key=00783295&item_key_date=810229&rid=GS [Accessed on 21/11/2020.].

[19] S. Kacianka and H. Hellwagner. Adaptive video streaming for uav networks. In *Proceedings of the 7th ACM International Workshop on Mobile Video*, 2015. https://doi.org/10.1145/2727040.2727043.

[20] S. Qazi and A. S. Siddiqui and A. I. Wagan. Uav based real time video surveillance over 4g lte. In *2015 International Conference on Open Source Systems Technologies (ICOSST)*, 2015. https://doi.org/10.1109/ICOSST.2015.7396417.

[21] Chengyi Qu, Alicia Esquivel Morel, Drew Dahlquist, and Prasad Calyam. Dronenet-sim: A learning-based trace simulation framework for control networking in drone video analytics. In *Proceedings of the 6th ACM Workshop on Micro Aerial Vehicle Networks, Systems, and Applications*, DroNet '20, New York, NY, USA, 2020. Association for Computing Machinery. https://doi.org/https://doi.org/10.1145/3396864.3399705.

[22] R. R. Ramisetty, C. Qu, R. Aktar, S. Wang, P. Calyam, and K. Palaniappan. Dynamic computation off-loading and control based on occlusion detection in drone video analytics. In *Proceedings of the 21st International Conference on Distributed Computing and Networking*, ICDCN 2020, 2020. https://doi.org/10.1145/3369740.3369793.

[23] DJI. Spark specs, 2020. [Online]. Available at:https://www.dji.com/de/spark/info#specs [Accessed on 11/01/2021.].

[24] DJI. Mavic air specs, 2020. [Online]. Available at:https://www.dji.com/de/mavic-air/info [Accessed on 11/01/2021.].

[25] Parrot. Parrot ar 2.0 elite edition, 2019. [Online]. Available at:https://www.parrot.com/global/drones/parrot-ardrone-20-elite-edition [Accessed on 20/05/2020.].

[26] Kismet. Kismet, 2021. [Online]. Available at:https://www.kismetwireless.net/ [Accessed on 11/01/2021.].

[27] Tcpdump. Man page of tcpdump, 2020. [Online]. Available at:https://www.tcpdump.org/manpages/tcpdump.1.html [Accessed on 11/01/2021.].

[28] A. Zolich, D. Palma, K. Kansanen, K. Fjørtoft, J. Sousa, K. H. Johansson, Y. Jiang, H. Dong, and T. A. Johansen. Survey on communication and networks for autonomous marine systems. *Journal of Intelligent & Robotic Systems*, 95(3):789–813, 2019. https://doi.org/10.1007/s10846-018-0833-5.

[29] DJI Developer. Onboard sdk documentation home, 2020. [Online]. Available at:https://developer.dji.com/onboard-sdk/documentation/introduction/homepage.html [Accessed on 11/01/2021.].

[30] S. Tanwir and H. Perros. A survey of vbr video traffic models. *IEEE Communications Surveys Tutorials*, 15(4):1778–1802, 2013. https://doi.org/10.1109/SURV.2013.010413.00071.

[31] D. A. Moltchanov. M/g/1 and m/g/1/k systems, 2013. [Online]. Available at:http://www.cs.tut.fi/~moltchan/ELT-53607/lecture07.pdf [Accessed on 11/01/2021.].

[32] H. Walidainy and Z. Zulfikar. An improved design of linear congruential generator based on wordlengths reduction technique into fpga. *International Journal of Electrical and Computer Engineering*, 5:55–63, 02 2015. https://doi.org/10.11591/ijece.v5i1.pp55-63.

[33] Huang, W. Lecture 19 - uniform and exponential distributions - text: A course in probability by weiss 8.4, 2014. [Online]. Available at:https://www.stat.purdue.edu/~huang251/handouts19.pdf [Accessed on 11/01/2021.].